

MOL #39867

The investigational anticonvulsant lacosamide selectively enhances slow inactivation of voltage-gated sodium channels

Adam C. Errington, Thomas Stöhr, Cara Heers & George Lees

Department of Pharmacology & Toxicology, Otago School of Medical Sciences, University of Otago, PO Box 913, Dunedin, New Zealand (A.C.E., G.L.) and Schwarz BioSciences GmbH, Department Pharmacology & Toxicology, Alfred Nobel Str. 10, 40789 Monheim, Germany (T.S., C.H.).

MOL #39867

Running title: Lacosamide enhances slow inactivation of sodium channels

Corresponding Author:

Professor George Lees PhD FRPharmS

Chair, Department of Pharmacology & Toxicology

Otago School of Medical Sciences

University of Otago

PO Box 913

Dunedin, New Zealand

Tel: 64 3 4797265

Fax: 64 3 4799777

e-mail: george.lees@stonebow.otago.ac.nz

Number of pages: 39

Number of tables: 0

Number of figures: 8

Number of references: 40

Number of words in abstract: 249

Number of words in introduction: 750

Number of words in discussion: 1500

Abbreviations: CBZ, carbamazepine; DPH, phenytoin; LTG, lamotrigine; LCM, lacosamide; HEPES, 4-(2-hydroxyethyl)-1-piperazineethansulphonic acid; EGTA, ethylene glycol-bis-(*b*-aminoethyl ether)-*N,N,N,N*-tetraacetic acid; SRF, sustained repetitive firing, VGSC, voltage-gated sodium channel, PHB, phenobarbital.

MOL #39867

Abstract

Our hypothesis was that lacosamide modulates voltage-gated sodium channels (VGSCs) at clinical concentrations (32-100 μ M). Lacosamide reduced spiking evoked in cultured rat cortical neurons by 30s depolarising ramps but not by 1s ramps. Carbamazepine and phenytoin reduced spike firing induced by both ramps. Lacosamide inhibited sustained repetitive firing during a 10 s burst but not within the first second. Tetrodotoxin-sensitive VGSC currents in N1E-115 cells were reduced by 100 μ M lacosamide, carbamazepine, lamotrigine and phenytoin from V_h : -60 mV. Hyperpolarization (500 ms) to -100 mV removed the block by carbamazepine, lamotrigine and phenytoin but not by lacosamide. The voltage dependence of activation was not changed by lacosamide. The inactive S-stereoisomer did not inhibit VGSCs. Steady state fast inactivation curves were shifted in the hyperpolarizing direction by carbamazepine, lamotrigine and phenytoin but not at all by lacosamide. Lacosamide did not retard recovery from fast inactivation in contrast to carbamazepine. Carbamazepine, lamotrigine and phenytoin but not lacosamide all produced frequency-dependent facilitation of block of a 3 s, 10 Hz pulse train. Lacosamide shifted the *slow* inactivation voltage curve in the hyperpolarizing direction and significantly promoted the entry of channels into the slow inactivated state (carbamazepine weakly impaired entry into the slow inactivated state) without altering the rate of recovery. Lacosamide is the only analgesic/anticonvulsant drug that reduces VGSCs availability by selective enhancement of slow inactivation but without apparent interaction with fast inactivation gating. The implications of this unique profile are being explored in phase III clinical trials for epilepsy and neuropathic pain.

MOL #39867

Introduction

Lacosamide (LCM, R-2-acetamido-*N*-benzyl-3-methoxypropionamide, also formerly known as Harkoseride, SPM 927 or ADD 234034, Fig 1A) is a novel anticonvulsant currently in phase III clinical trials that has shown significant promise in the treatment of partial seizures with or without secondary generalization (Doty et al., 2007) and diabetic neuropathic pain (McCleane et al., 2004). In pre-clinical screens, the functionalised amino acid molecule was more potent than both phenytoin (DPH) and phenobarbital (PHB) in preventing tonic hind limb extension in the maximal electroshock seizure (MES) test *in vivo* in both rats (ED_{50} = 3.9 mg/kg p.o.) and mice (ED_{50} = 4.5 mg/kg i.p.) (LeTiran et al., 2001). LCM was also anticonvulsant in two animal models for *status epilepticus* and showed a high degree of stereoselectivity (the S-stereoisomer SPM 6953 was 10-30 times less potent in the MES test) (LeTiran et al., 2001).

The molecular mode of action of LCM is still unknown. Binding studies have revealed that LCM does not displace radioligands from a plethora of recognised anticonvulsant receptor/channel binding sites, including those for NMDA (PCP, MK-801, glycine), AMPA, GABA_A, GABA_B, 5-HT and dopamine (Errington et al., 2006). In electrophysiological studies LCM (100 μ M) did not affect currents evoked by application of exogenous NMDA, AMPA or GABA in cortical neuronal cultures, but did significantly reduce the incidence of both spontaneous inhibitory postsynaptic currents (IPSCs) and excitatory postsynaptic currents (EPSCs), as well as producing inhibition of spontaneously firing action potentials (Errington et al., 2006). This early data suggested that LCM does not interact with known recognition sites for anticonvulsants on ligand-gated ion channels or other synaptic receptors.

As previously disclosed, LCM has shown significant potency in the MES test *in vivo* and a relative lack of efficacy in the threshold pentylenetetrazol (PTZ) model. This profile is similar to the antiepileptic drugs carbamazepine (CBZ), lamotrigine (LTG) and DPH, all of which are

MOL #39867

selective for the former experimental seizure model over the latter (Meldrum, 2002; Lang et al., 1993; Miller et al., 1986). It is now generally accepted that CBZ, LTG and DPH share a common primary mode of action (although postulated novel molecular target sites may contribute to the distinct pharmacological profiles of the drugs in different cellular compartments; Cunningham et al., 2000; Poolos et al., 2002; Ridall et al., 2006) in altering fast inactivation gating of voltage gated sodium channels (Lang et al., 1993; Willow et al., 1985; Ragsdale et al., 1996) producing tonic and use dependent blockade.

In our earliest mechanistic studies, sustained repetitive firing (SRF; 750 ms) evoked by somatic current injection was weakly, but significantly, reduced in frequency by LCM without apparent changes (amplitude, duration) in individual spike properties (Errington et al., 2006). The subtle reduction in the number of spikes throughout a 750 ms period of SRF by LCM was markedly different to that produced by acknowledged sodium channel blocking anticonvulsants. These older drugs typically produce complete block of regenerative spiking within a few tens of milliseconds of an evoked SRF burst (Lees and Leach, 1993; Wang et al., 1993; Lang et al., 1993; Willow et al., 1985; McLean and McDonald, 1986). Nonetheless, the marginal effect of LCM on electrogenesis in this experiment may suggest that the novel anticonvulsant could be acting, in part, via inhibition of VGSCs. This postulate was reinforced by binding data that showed LCM (10 μ M) was capable of producing 25 % displacement of [3 H]-batrachotoxin binding to VGSC site 2 in rat brain homogenates (Errington et al., 2006). Our earlier experiments suggested that the drug could interfere preferentially with seizure spread, could reduce synaptic traffic (indiscriminately for excitation and inhibition) and spontaneous action potentials and that voltage gated potassium and calcium channels were not targeted (Lees et al., 2006; Errington et al., 2006). On the basis of these leads, in this paper we have examined the hypothesis that LCM may be a modulator of VGSC but that it may require different biophysical conditions (or exploit a new

MOL #39867

target site) to produce inhibition compared to existing anticonvulsant drugs in the pharmacopoeia (CBZ, LTG and DPH) which have been used for comparison. We report that LCM does not modify fast inactivation of the VGSC like the other VGSC modulating anticonvulsants but that it has a unique inhibitory action in promoting slow inactivation of the VGSC (a new mechanism for blocking a target acknowledged for its importance in the treatment of epilepsy and pain). The implications of this novel mechanism for the pharmacological profile of the drug are unknown but are currently being characterised in ongoing clinical trials.

MOL #39867

Materials and Methods

Primary neocortical neuron culture

Neuronal cultures were prepared from cerebral cortices of E16-18 Sprague Dawley rats. Donor animals were humanely killed and embryos were collected by caesarian section in accordance with Schedule 1 of the Home Office Animals (Scientific Procedures) Act, UK, 1986 and with the approval of University of Otago Animal Ethics committee. Cortices were minced with a razor blade and dissociated by trituration through Pasteur pipettes (without the addition of proteolytic enzymes). Isolated cells were plated onto poly-D-lysine coated glass shards (approximately 40 mm²) at densities between 50,000 and 100,000 cells ml⁻¹ in Neurobasal medium (Invitrogen, UK) containing 2% B27 (Invitrogen, UK), 1 % Glutamax-1™ (Invitrogen, UK), 100 U/μg per ml penicillin/streptomycin (Sigma, UK) and 25 μM L-glutamate (Sigma, UK) as previously described (Errington et al., 2006). Cells were maintained in a humidified incubator at 37 °C and 5 % CO₂. After 3 days *in vitro* (DIV) 50 % of the media was removed and replaced with twice the volume of fresh media as defined above but without L-glutamate. After 7 DIV a further feed was given to allow maintenance of viable cultures for several weeks. Cells were used in experiments typically after 21-28 DIV.

N1E-115 Mouse neuroblastoma cell culture

N1E-115 mouse neuroblastoma cells were obtained from the European Collection of Animal Cell Cultures (ECACC, Wiltshire, UK). Confluent cells (70-80 %) were subcultured twice weekly and grown on poly-D-lysine coated glass shards in Dulbecco's Modified Eagle Medium (DMEM, Invitrogen, UK) containing 10 % fetal calf serum (Sigma, UK) and 100 U/μg per ml penicillin/streptomycin (Sigma, UK). Cells were incubated at 37 °C in 5 % CO₂ in triple vented 35 mm cell culture dishes (Iwaki, Japan). Cells were used for electrophysiological experiments 24-48 hrs after plating.

MOL #39867

Electrophysiology

Cultured neurons adhering to glass shards were placed in a Perspex trench on the stage of a Nikon Diaphot (Nikon, Japan) inverted phase contrast microscope and superfused (circa 2 ml min⁻¹) with buffered physiological saline containing (mM) NaCl 142; KCl 2.5; CaCl₂ 2; MgCl₂ 1; HEPES 10; D-glucose 30; pH 7.4 (NaOH). Recordings were made from neurons of pyramidal morphology (unless otherwise stated) using the whole-cell patch clamp technique with intracellular solution consisting of (in mM) K-gluconate 142; CaCl₂ 1; MgCl₂ 2; HEPES 10; EGTA 11; pH 7.4 (KOH). Micropipettes were fabricated on a model P97 Flaming/Brown Micropipette puller (Sutter Instrument Co, USA) using GC150T-10 borosilicate glass (Harvard Apparatus Ltd, UK) resulting in pipettes with an impedance of typically 4-5 MΩ. All patch clamp recordings were performed at room temperature (~ 22 ± 1 °C) using an Axopatch 200 integrating amplifier (Axon Instruments, USA). For sustained repetitive firing experiments 2mM CoCl₂ and the AMPA receptor antagonist 6-cyano-7-nitroquinoxaline-2,3-dione (CNQX, 10 μM) were added to the bath to prevent calcium entry and recurrent excitability.

For voltage clamp experiments on N1E-115 cells the bath was continuously perfused with a solution containing (mM): NaCl 140; KCl 5; CaCl₂ 1.8; MgCl₂ 0.8; HEPES 10; pH 7.3 (NaOH) at a flow rate of approximately 1.5-2 ml.min⁻¹. Patch pipettes (3-5 MΩ) were filled with solution containing (mM) NaCl 10; TEA-Cl 20; CsCl 110; CaCl₂ 1; MgCl₂ 2; EGTA 11; HEPES 10; pH 7.4 (CsOH). In order to reduce the capacitance of the microelectrode, filled glass pipettes were immersed in Sigmacote (Sigma, UK) or coated with Sylgard 184 (Dow Corning, USA). Isolated, spherical and unclumped neuroblastoma cells were selected for patch clamp experiments (to minimise space clamp problems) and whole cell capacitance and series resistance were cancelled using the preamplifier. 70-85 % series resistance compensation was routinely applied. To allow accurate measurement of I/V properties, 5

MOL #39867

minutes was allowed after membrane rupture to achieve full dialysis of the cell before data was recorded. Series resistance was monitored throughout all experiments and cells were discarded if it became greater than three times the open pipette resistance (*circa* 15 M Ω). Pulse protocols were applied in control solutions and again after 3 minutes equilibration with drugs unless otherwise indicated.

Data were filtered at 5 kHz and digitised at 15 - 20 kHz using a CED *micro1401* (Cambridge Electronic Design, UK) and pulse protocols were generated using Signal 2.10 (CED, UK) software. To isolate pure ionic currents through sodium channels, leak currents and residual capacitance artefacts were deducted offline using Signal software. For activation curves, conductance (g) through Na⁺ channels was calculated by $g = I_{Na^+} / (V - E_r)$ where I_{Na^+} is the peak sodium current, V is the test potential and E_r is the observed reversal potential. Activation and inactivation curves were fitted to a Boltzmann function of the form:

$$(g/g_{max}) = 1/(1 + \exp[(V_{50} - V)/k]) \text{ or } (I/I_{max}) = 1/(1 + \exp[(V_{50} - V)/k]) \quad (1)$$

where g_{max} is the peak conductance, I_{max} is the peak current, V_{50} is the voltage at which half maximal current/conductance occurs, k is the slope factor and V is the test potential. Recovery from steady-state fast inactivation was best fit with a bi-exponential equation of the form:

$$I_{Na}(t) = A_1(1 - \exp(-\tau_1 * t)) + A_2(1 - \exp(-\tau_2 * t)) \quad (2)$$

where t is time, A is the amplitude component of each exponent and τ is time constant for recovery. Slow inactivation voltage curves were fit using a modified Boltzmann equation (Carr et al., 2003) of the form:

MOL #39867

$$I/I_{\max} = (1 - I_{\text{resid}})/(1 + \exp(-(V_m - V_s)/k)) + I_{\text{resid}} \quad (3)$$

Details of specific pulse protocols are described in the results text or figure legends. All data are depicted as mean \pm standard error of the mean (SEM) and statistical analysis was by one-way ANOVA (Dunnett's post *hoc*), paired/unpaired *t*-test, Mann-Whitney test or Kruskal-Wallis (Dunn's post *hoc*) test where appropriate.

Pharmacology

All reagents were obtained from Sigma UK unless otherwise indicated. For electrophysiological experiments CBZ and DPH were obtained from Sigma, UK and LTG from Tocris Cookson, UK. All drugs were formulated daily by dissolution into dimethylsulphoxide (DMSO, Sigma). The final concentration of DMSO in physiological solutions was not greater than 0.1 % V/V and all drug-free control solutions contained an equal concentration of the solvent. LCM and SPM 6953 were supplied by Schwarz Pharma GmbH (Monheim, Germany).

MOL #39867

Results

Electrophysiology: Primary neocortical neurons

Sodium spikes evoked by fast or slow depolarising ramps are differentially sensitive to anticonvulsants

To study the effects of LCM upon electrogenesis, cultured rat cortical neurons were voltage clamped in physiological saline using a K^+ -gluconate based intracellular solution. From a holding potential of -70 mV a slow depolarising (3 mV/sec) voltage ramp to +20 mV was applied to the cell soma through the patch pipette. In a subpopulation of neurons tested, as the result of space clamp complications caused by the extensive neuritic projections present in the mature cultured neurons, adequate voltage clamp could not be maintained in response to the depolarising ramp. The lack of control over the cellular potential consequently lead to firing of high frequency trains of action currents mediated by TTX-sensitive voltage gated sodium channels (Fig. 2). From an electrophysiological stand-point this would usually be considered undesirable. From a pharmacological perspective it allowed us to examine the effects of drugs on membrane excitability in response to slow and sustained depolarisation. LCM could profoundly inhibit the firing of action currents that were induced by this slow ramp depolarisation protocol. In drug-free control solutions slow ramps evoked 50.25 ± 10.25 spikes per burst ($n = 4$) and this was reduced to 13.50 ± 6.74 (76.54 ± 8.91 % reduction, Fig. 2CD) spikes per burst after 3 minutes perfusion with LCM (100 μ M, $P < 0.05$, Kruskal-Wallis), an effect that was reversible upon washout (46.75 ± 7.00). Both CBZ (fast binding, Kuo et al., 1997) and DPH (slowly binding, Kuo and Bean, 1994) could almost completely occlude the firing of spikes in response to the slow ramps with 99.67 ± 0.33 % ($n = 4$) and 98.75 ± 1.08 % ($n = 4$) reduction respectively (Fig. 2CD). However, in a similar suite of experiments where the rate of potential change was much more rapid (90 mV/sec) the

MOL #39867

resulting trains of evoked spikes were insensitive to LCM. In control solutions depolarisation by such a ramp induced the firing of 10.50 ± 1.99 spikes per burst whereas in the presence of LCM this was only very marginally ($P > 0.05$, $n = 10$) reduced to 9.30 ± 2.17 (17.91 ± 9.47 % reduction). This depolarisation-rate dependent block of bursts by LCM appeared to reinforce previous observation of only very marginal inhibition of brief (750 ms) sustained repetitive firing by LCM (Errington et al., 2006). Furthermore, the spikes evoked by the rapid depolarising ramp were still highly sensitive to the fast inactivation modifying drugs CBZ and DPH ($n = 4$) which produced 78.76 ± 6.00 % and 75.87 ± 14.26 % reduction respectively (Fig. 2AB). When the potential was ramped rapidly LCM did not increase the latency to the first spike, in fact a small reduction in time to first spike was observed compared to control (-1.04 ± 1.29 %, Fig. 2AB). In contrast, both CBZ and DPH produced increased latency to first spike compared to control ramps with 10.53 ± 10.26 % and 3.57 ± 2.60 % increase respectively.

Prolonged sustained repetitive firing is markedly attenuated by lacosamide but with slow kinetics compared to other anticonvulsants

Ictal-seizures and epileptiform paroxysmal depolarising shifts (*in vitro* and *in vivo*) often last for tens of seconds to minutes so we decided to test the ability of LCM to block prolonged SRF bursts (in contrast to brief 750 ms pulses previously studied, Errington et al., 2006). Ten seconds of sustained repetitive firing was evoked in current clamped ($E_{rest} -61 \pm 1.5$ mV, $n = 16$) cortical neurons. Previous experiments, in a brain slice model of tonic-clonic epileptiform activity induced by 4-AP (Lees et al., 2006), showed that LCM markedly reduced the duration of prolonged tonic firing. The mean firing frequency over the entire 10 second burst (10 s bins) was calculated from the average of four pre-treatment or drug treated (5 minute bins) bursts (Fig. 3). In the absence of drugs, neurons produced high frequency (15.04 ± 0.94 Hz) trains of overshooting (First AP overshoot: 65 ± 3.1 mV, $n = 16$) action potentials. Neither

MOL #39867

E_{rest} nor overshoot of the first action potential (LCM 320 μ M: -64 ± 9.5 mV; CBZ 100 μ M: -65 ± 4.1 mV) were significantly ($P > 0.05$, Mann Whitney) affected by LCM (32-320 μ M) or CBZ (100 μ M). Perfusion of the cellular monolayer with LCM produced a significant concentration dependent (EC_{50} : 48 μ M) reduction in the mean firing frequency of neurons compared to pre-treatment, an effect that was fully reversible upon washout (Fig. 3 A-C). At 32 μ M LCM produced a noticeable, but not significant, reduction in the mean firing frequency (CONTROL: 12.86 ± 0.84 Hz; LCM: 9.32 ± 0.94 Hz, $P > 0.05$, $n = 4$, Wilcoxon matched pairs). When the concentration was increased to 100 μ M the drug significantly inhibited sustained firing (CONTROL: 16.25 ± 1.6 Hz; LCM 2.63 ± 0.43 Hz, $P < 0.01$, $n = 9$) and this was enhanced further with an increase in concentration to 320 μ M (CONTROL: 14.6 ± 1.18 Hz; LCM 1.28 ± 0.19 Hz, $P < 0.01$, $n = 4$). However, the temporal characteristics of the block showed that residual spikes occurring in the presence of the drug are confined to the initial segment of the burst. When the prolonged SRF bursts were analysed in 1 second bins the data showed that LCM did not profoundly inhibit the firing rate of action potentials within the early phase of the burst (EC_{50} : 640 μ M). Even at 320 μ M LCM only produced $27.1 \pm 1\%$ reduction in firing frequency and allowed residual high frequency burst activity of 0.68 ± 0.07 s duration. Unlike the effects of LCM, the fast inactivation modifying anticonvulsants CBZ, LTG and DPH all produced a marked reduction of firing frequency well within the first second of the burst. 100 μ M CBZ ($n = 4$, Fig. 3D-E) blocked all spikes except those occurring in the first 0.11 ± 0.006 s of the SRF burst and this was accompanied by a dramatic attenuation of the amplitude or full occlusion of the remaining action potentials. Although the data for LTG and DPH were not quantitatively analysed they were qualitatively similar to the fast effects of CBZ on prolonged SRF bursts (Fig. 3E). LCM clearly inhibits the firing of repetitive action potentials and reduces cellular excitability although it is clear that, unlike CBZ, LTG and DPH relatively prolonged depolarisation is required before the block is

MOL #39867

apparent. The inability of even 320 μM LCM to inhibit the early phase of SRF (Fig. 3D) is strongly indicative that the marked divergence between LCM and CBZ / LTG / DPH on SRF (and bursts evoked by ramps) does not simply reflect difference in potency at a common target site. The characteristics of the inhibition produced by the novel drug suggest that it may be binding to a different binding site or that the binding rates are significantly slower than for the existing clinically used molecules.

Electrophysiology: Mouse N1E-115 neuroblastoma cells

Lacosamide inhibits voltage activated sodium currents

Mouse neuroblastoma cells were patch clamped in the whole cell configuration. All cells showed fast, rapidly-inactivating inward currents in response to step depolarisation. Peak currents were evoked by 10 ms depolarising steps to varying test potentials (-70 to 100 mV) from a holding potential (V_h) of -60 mV preceded by a 500 ms hyperpolarizing step to -100 mV to remove the influence of fast inactivation (Fig. 4B). The evoked-currents were fully blocked by 500 nM TTX (Fig. 4A inset) but were insensitive to 500nM Cd^{2+} (not shown) and the kinetics, activation- and reversal-potentials (Fig. 4) were consistent with fast channels selective for Na^+ . Application of 100 μM LCM to the clamped cells resulted in a reduction in the peak sodium current observed at all test potentials (Fig. 4AB). The maximal current evoked in response to a 10 ms test pulse to 0 mV was 0.61 ± 0.02 (n = 4) that of control in the presence of LCM and the effects were fully reversible following removal of the drug (Fig. 4B) Inhibition of sodium currents by LCM was not accompanied by shifts in the voltage dependence of activation gating for the channels (V_{50} : CONTROL -5.3 ± 4.0 , k : 8.1 ± 1.5 , n = 4; LCM -4.2 ± 3.7 , k : 8.8 ± 1.8 , n = 4; $P > 0.05$, Fig. 4C) and did not alter the reversal potential (although this was not analysed in detail). In contrast to this the S stereoisomer,

MOL #39867

SPM 6953 at the same concentration marginally increased the fraction of available current (1.11 ± 0.03 , $n = 4$, $P > 0.05$, Fig. 4D).

Inhibition of sodium currents by lacosamide shows markedly different voltage dependent properties compared to other antiepileptic drugs.

To test the voltage dependence of block, neuroblastoma cells were maintained at a holding potential of -60 mV and depolarised by a 10 ms test pulse to 0 mV at 0.5 Hz. The protocol was repeated in each cell with a 500 ms hyperpolarizing pulse to -100 mV prior to the depolarising test pulse (Fig. 5A). In all cells tested ($n \geq 4$) all four of the anticonvulsant drugs (100 μ M) produced a reduction in current when V_h was -60 mV (Residual current following drug equilibration was for CBZ 0.29 ± 0.17 , $n = 4$ Fig. 5B; LTG 0.50 ± 0.08 , $n = 5$ Fig. 5B; DPH 0.52 ± 0.10 , $n = 6$ Fig. 5B; LCM 0.68 ± 0.05 , $n = 7$ Fig. 5AB). For CBZ, LTG and DPH application of a 500 ms hyperpolarizing pulse to -100 mV significantly (two tailed unpaired t -test) reduced the blocking action on the channel, with the fraction available being 0.94 ± 0.19 ($P < 0.05$); 0.88 ± 0.06 , ($P < 0.01$); and 0.99 ± 0.05 ($P < 0.01$) respectively compared to control values. The inhibition produced by LCM was not ($P > 0.05$) altered by the hyperpolarizing prepulse. When 500 ms prepulses to -100 mV were applied in the presence of LCM, the peak, evoked current was still reduced to 0.71 ± 0.06 of the pre-treatment maximum (Fig. 5AB)

Rapid frequency dependent facilitation of block is not observed with lacosamide

A series of 30 test pulses (20 ms to 0 mV) were delivered from a holding potential of -80 mV at 10 Hz. The available current in control and in the presence of drugs was calculated by dividing the peak current at any given pulse (pulse_n) by the peak current in response to the initial pulse (pulse_1). CBZ (0.80 ± 0.01 , $P < 0.01$, $n = 6$), LTG (0.84 ± 0.01 , $P > 0.05$, $n = 7$)

MOL #39867

and DPH (0.78 ± 0.01 , $P < 0.001$, $n = 7$) markedly reduced current amplitude compared to controls (0.90 ± 0.01 , $n = 10$) by the tenth pulse in the train but the LCM currents were almost superimposable with controls (Fig. 5C-D). Interestingly, LCM began to show some degree of use dependent block, with a distinct latency, only after approximately 13-14 test pulses, (Fig. 5D *arrow*). However, even by the last of the 30 pulses delivered the peak current available was still not significantly different from control (CONTROL 0.89 ± 0.01 ; LCM 0.83 ± 0.01 , $P > 0.05$). In contrast by the thirtieth test pulse in the train in the presence of CBZ (0.78 ± 0.01 , $P < 0.01$), LTG (0.79 ± 0.01 , $P < 0.05$) or DPH (0.71 ± 0.02 , $P < 0.001$) the available peak current was significantly reduced compared to control.

Steady state fast inactivation voltage curves were not shifted in the hyperpolarizing direction by lacosamide.

Steady state fast inactivation curves (Fig. 6A) were fit to a single Boltzmann function of the form described previously (equation 1). The protocol (Fig. 6A *inset*) was designed with the intention of recruiting predominantly fast sodium channel inactivation and minimising the development of slowly inactivated conformations. The V_{50} for inactivation under control conditions was -66 ± 0.9 mV ($n = 21$, pooled from all replicates). Significant hyperpolarizing shifts in the inactivation curves (summary statistics in Fig. 6C) were produced by CBZ (V_{50} : -79 ± 2.6 mV; $n = 5$, $P < 0.001$, Fig 6AB), LTG (V_{50} : -72 ± 1.7 mV, $n = 7$, $P < 0.05$, Fig. 6B) and DPH (V_{50} : -77 ± 2.3 mV, $n = 7$, $P < 0.05$, Fig. 6B). LCM (100 μ M) did not produce a significant shift in the V_{50} for inactivation of sodium currents in the neuroblastoma cells. The voltage for half maximal inactivation after equilibration with LCM (-65 ± 1.7 mV, $n = 7$, Fig 6D) was not significantly different ($P > 0.05$) to the observed V_{50} in control solutions. It is noteworthy that, in contrast to the fast inactivation modifiers, the entire curve for the experiments in the presence of LCM displayed a very marginal depolarising shift although

MOL #39867

this was not significant. Furthermore, the slopes (k) of the inactivation curves were decreased marginally by CBZ (k : 7.1 ± 0.6 mV, $P > 0.05$), DPH (k : 7.3 ± 0.2 mV, $P > 0.05$) and significantly by LTG (k : 7.5 ± 0.3 mV, $P < 0.05$) whilst the slope in the presence of LCM was almost identical to the control value (k : 6.6 ± 0.3 mV, Fig. 6B).

Lacosamide does not significantly retard the recovery of sodium channels from steady state fast inactivation.

Neuroblastoma cells were held at -90 mV and a test pulse to -10 mV (20 ms) was given prior to a conditioning pulse of 500 ms to the same potential. After the conditioning pulse, varying time for recovery (Δt) was allowed before delivery of a second test pulse (Fig. 6D). The holding potential and relatively brief conditioning pulses were designed to remove the potential influence of sodium channel slow inactivation and isolate the fast inactivation gating process. The fraction of current available after each recovery period (depicted Fig. 6E) is the result of the second test pulse divided by the first. In control conditions a relatively large proportion of the sodium current (0.41 ± 0.03 , $n = 7$, Fig. 6DF) was re-available after only a brief recovery period (3ms, 50 % maximal recovery ~ 4 ms). When $100 \mu\text{M}$ CBZ was applied to the bath for three minutes prior to running the pulse protocol the fraction available after 3 ms was significantly reduced ($P > 0.001$, $n = 5$, Fig. 6DEF) to 0.18 ± 0.03 (50 % maximal recovery ~ 37.5 ms). LCM on the other hand did not produce any significant ($P > 0.05$, $n = 5$) retardation in recovery of channels from steady state fast inactivation with the fraction available at 3 ms being 0.40 ± 0.04 (50 % maximal recovery circa 4.3 ms). In response to the 500 ms conditioning potential used CBZ but not LCM, was able to inhibit the recovery of sodium channels from fast inactivation for up to 300 ms after repolarisation (as summarised in Fig. 6F).

MOL #39867

Lacosamide enhances the entry of sodium channels into the unavailable slow inactivated state

In light of the ability of LCM to inhibit sodium currents despite any apparent effect upon fast inactivation gating we decided to assess the effect of the novel drug upon voltage gated sodium channel slow inactivation. In line with the findings of many authors in a varied range of preparations, VGSCs in the mouse N1E-115 cells undergo the physiological process of slow inactivation when exposed to periods of prolonged depolarisation. To assess the entry of sodium channels into the slowly inactivated state, cells were held at -80 mV and depolarised for either 10 or 30 seconds to -10 mV, followed by a recovery interval of 1.5 s, prior to a test pulse to measure the peak available current (Fig 7A *inset*). The recovery interval of 1.5 s was used to completely allow the recovery of fast inactivation making occupancy of the slow inactivated state the sole determinant of the second test pulse amplitude. When neuroblastoma cells were depolarised for 10 seconds the peak available current was reduced to 0.73 ± 0.01 ($n = 18$, pooled from all experiments described below) that of the preconditioning test pulse and when the conditioning pulse was increased to 30 seconds duration the current available was reduced further to 0.61 ± 0.02 ($n = 4$).

LCM enhanced the entry of sodium channels into the slow inactivated state in a concentration dependent manner. Under control conditions the degree of physiological slow inactivation induced by the conditioning pulse was consistent ($P > 0.05$, Fig. 7B open circles) across three different groups of cells. $32 \mu\text{M}$ LCM produced a slight, but not significant ($n = 5$, $P > 0.05$, paired t test), increase in the fraction of channels that became unavailable due to slow inactivation with 0.63 ± 0.05 available compared to pre-treatment value of 0.69 ± 0.05 (Fig. 7AB). However, when the concentration of LCM was increased to $100 \mu\text{M}$ a significant reduction in the fraction of available channels was noted after the conditioning pre-pulse. The fraction of channels available was reduced to 0.50 ± 0.02 compared to 0.73 ± 0.02 in the same cells prior to LCM application ($n = 6$, $P < 0.01$, Fig. 7AB). $320 \mu\text{M}$ LCM significantly ($P <$

MOL #39867

0.001, $n = 7$) reduced the fraction of available channels to 0.38 ± 0.01 compared to 0.71 ± 0.02 pre-treatment. Plots of normalised peak current (P2/P1, Fig. 7D) against conditioning pulse duration were fit with a mono-exponential function and yielded a time constant for the physiological entry into slow inactivation (for the pulse protocol used) of $\tau_{\text{ctrl}} = 11.95$ s (Fig. 7 D). LCM (100 μM) more than doubled the reduction of sodium channel availability that resulted from entry into the slow inactivated state. In the presence of the drug using the pulse protocol shown, channels entered the slow inactivated state with a time constant for entry of $\tau_{\text{LCM}} = 4.79$ s. The highly significant, concentration-dependent and reversible (not shown) LCM-induced changes were measured over a limited number of data points which prevented a deeper kinetic analysis of the LCM induced acceleration of entry into the slowly inactivated state.

Moreover, LCM was able to produce tonic inhibition of transient sodium currents at -80 mV but the affinity of the channel for the drug was low with an EC_{50} of 569 ± 1.2 μM ($n = 5-7$; Fig. 7C). When the conditioning pulse to -20 mV for 10 s was applied, the affinity of the drug for the channel was markedly increased with an EC_{50} for inhibition of 164 ± 1.2 μM . These values are likely to underestimate the true dissociation constant of channels in both the resting and slowly inactivated states. If cells were held at very negative potentials (-120 mV) for periods exceeding the time constant for entry into slow inactivation (several tens of seconds which was not possible for technical reasons) it is likely that the EC_{50} for LCM would be even greater than that quoted (at -80 mV).

The slow inactivation voltage curve is shifted to more hyperpolarized potentials by lacosamide

To test the voltage dependence of the slow inactivation process in N1E-115 cells the pulse protocol shown in the inset in Figure 8A was used. Using this protocol, physiological slow inactivation became prevalent at potentials more depolarised than -80 mV but was only 30 %

MOL #39867

complete at the maximum conditioning pulse of -10 mV ($n = 7$, Fig. 8AB). The inactivation voltage curve was fit using a modified Boltzmann function (equation 3), but the relatively small fraction of slow inactivation induced meant that the estimated potential for half maximal reduction of channel availability (V_{50}) under control conditions was circa $+64$ mV. LCM significantly ($P < 0.01$, Friedman test, $n = 7$) shifted the slow inactivation voltage curves to more hyperpolarized membrane potentials in a concentration dependent manner (Fig. 8A). In the presence of 100 μ M LCM the curve was shifted significantly with half maximal reduction in channel availability at -57 ± 4.5 mV ($n = 4$). The first significant change in channel availability in the presence of 100 μ M LCM was noted at a conditioning potential of -80 mV; more hyperpolarized than the typical resting potential of many neurons. LCM application also significantly increased the maximal fraction of current made unavailable by depolarisation (-10 mV, CONTROL 0.70 ± 0.02 , $n = 7$, LCM 0.41 ± 0.04 , $n = 4$, $P < 0.01$, Mann Whitney test).

Lacosamide does not alter the rate of recovery of channels from the unavailable slow inactivated state.

Although LCM enhanced entry to slow inactivation and reduced the fraction of channels available after a long conditioning pulse, the half life for recovery of the channels from the slow-inactivated state was not significantly altered by the drug. The rate of recovery of channels from slow inactivation was measured using the protocol shown in Figure 8B (*inset*). After a 10 second conditioning pulse to -20 mV a fraction of the current was made unavailable for activation by a second test pulse as previously described. Under control conditions the half-life for recovery of the current back to steady state maximal was 5.8 ± 0.5 s (mono-exponential fit, $n = 6$). When LCM (100 μ M) was applied for three minutes, a proportion of the current was unavailable (prior to conditioning pulse, $V_h = -80$ mV) and the

MOL #39867

fraction made unavailable by the conditioning pulse was enhanced. The rate at which the unavailable channels recovered and became available for activation was not significantly altered by LCM ($P = 0.17$) with the half life for recovery from slow being 6.7 ± 0.3 s (Fig. 8B). When the conditioning pulse was extended to 30 seconds duration the fraction of current made unavailable by physiological slow inactivation was greater than that resulting from a 10 second pulse. The kinetics of physiological channel recovery was marginally slower for the longer conditioning pulse with a half life of 7.8 ± 0.6 s ($n = 4$, not shown). As with the shorter conditioning pulse LCM produced tonic inhibition of the evoked sodium current and increased the fraction made unavailable by conditioning. Again however, the half-life for recovery of the channels was not significantly altered in the presence of the anticonvulsant (9.1 ± 0.3 s, $P = 0.09$, not shown). In marked contrast to the effects of LCM upon slow inactivation observed using this protocol, in three of three neuroblastoma cells tested, CBZ did not enhance the fraction of channels made unavailable by a prolonged depolarising pulse. In contrast, a slight, but not significant ($P > 0.05$, Wilcoxon Matched Pairs) reduction in the fraction of channels made unavailable by slow inactivation was noted in the presence of $100 \mu\text{M}$ CBZ (0.89 ± 0.03 , $n = 3$) compared to control measurements (0.79 ± 0.06 , $n = 3$, Fig. 8C). CBZ did not significantly alter the kinetics of channel recovery from slow but the half-life for this recovery process was reduced by the drug (control half life 6.4 ± 1.3 s; CBZ 3.0 ± 0.8).

MOL #39867

Discussion

We have shown that currents through VGSCs of CNS neurons are sensitive to inhibition by the novel anticonvulsant LCM. The inhibitory actions produced by LCM are mechanistically distinct from those seen with VGSC fast inactivation modifiers. Reduction of sodium currents, through binding to a high affinity receptor site that becomes available during depolarization (Ragsdale et al., 1996; McPhee et al., 1995; Ragsdale and Avoli, 1998; Kuo, 1998), plays a major part in the anticonvulsant actions of CBZ, DPH and LTG. This high affinity binding site, or ‘modulated receptor’, is located between the outer pore lining regions of IIIS6 and IVS6, in particular the amino acid residues F1764 and Y1771. In line with the ‘modulated receptor’ hypothesis when neuroblastoma cells were held at a potential of -60 mV (where steady state fast inactivation is prevalent) CBZ, LTG, DPH and LCM all produced significant impairment of the fast transient sodium current.

As inhibition of I_{Na} by CBZ, LTG and DPH follows the voltage dependence of steady state inactivation gating it was impeded, to a large extent, when 500 ms hyperpolarizing pulses to -100 mV were applied prior to test pulses. This is unsurprising in light of the fact that recovery from steady state fast inactivation was approximately 90% complete after only 300 ms in the presence of CBZ. Inhibition of I_{Na} by LCM was not eroded by a hyperpolarizing prepulse delivered in advance of the test pulse. This suggested that the inhibition produced by the novel drug was not dependent upon the exposure of the so-called ‘modulated receptor’, as is the case for CBZ, DPH and LTG. Further evidence supporting this postulate was the lack of any hyperpolarizing shift in the steady state inactivation curve under conditions where the peak sodium current was significantly inhibited by LCM. This was in marked contrast to the significant shifts (in V_{50}) produced by acknowledged fast inactivation modifiers. We saw a greater shift in the V_{50} for steady state inactivation produced by CBZ over DPH and LTG reflecting the more rapid binding rate of the former over the latter to the inactivated channel.

MOL #39867

Despite using relatively short conditioning pulses (500 ms) DPH and LTG, whose on-binding rates to the inactivated channel are low (Kuo and Lu, 1997; Kuo and Bean, 1994), still produced significant hyperpolarizing shifts. In our experiments, inhibition of sodium currents by LCM appeared largely dependent upon tonic holding potential (-70 mV) and was not greatly accentuated or reversed by brief (500 ms) depolarising or hyperpolarizing pulses.

Drugs that bind to voltage-dependent conformations of VGSCs generally demonstrate frequency dependent facilitation of block (Lang et al., 1993; Willow et al., 1985; Vedantham and Cannon, 1999). In response to a train of depolarising pulses (10 Hz) from a holding potential of -80 mV, the probability of channels occupying the inactivated state is dramatically increased and rapid cumulative block was observed with CBZ, LTG and DPH. We did not see the characteristic response observed with fast inactivation modifying anticonvulsants when we tested LCM using this protocol. In contrast the inhibition of sodium currents by LCM showed a slowly developing facilitation of block that was only apparent after several pulses (1-1.5 s). Furthermore, during prolonged episodes of sustained repetitive firing, in complete contrast to CBZ, LTG and DPH, LCM was only able to facilitate spike failure after a similar temporal lag. Two plausible mechanisms may explain these findings. We cannot discount the possibility of a high affinity, ultra-slow binding interaction of the novel drug with a target site on the channel protein that becomes exposed for liganding rapidly during depolarization. For example it is known that CBZ binds to the fast inactivated channel with 3 fold lower affinity than DPH but that the rate of binding is five times faster (Kuo and Bean, 1994; Kuo et al., 1997). The slow onset of inhibition by LCM may ultimately be the result of slow association (binding) to the fast inactivated (gating transition) channel or to transition states along the activation pathway which underpin frequency dependent block by local anaesthetics (Vedantham and Cannon, 1999). If this is the case however, our results demonstrate a rate of binding that is dramatically slower than existing anticonvulsant drugs. A

MOL #39867

second, and perhaps a more likely explanation (based on our findings), is that LCM may be reducing the availability of sodium channels by enhancing the intrinsic inhibitory physiological mechanism of slow inactivation via a novel binding site.

Slow inactivation of VGSCs was first discovered in squid axon (Rudy, 1978) and subsequently in mammalian preparations including hippocampal neurons (Jung et al., 1997; Mickus et al., 1999) and neuroblastoma cells (Quandt, 1988). It involves a presumptive structural channel rearrangement that develops over several hundreds of milliseconds to seconds (roughly 100 – 1000 fold greater than fast inactivation) of sustained depolarization (Toib et al., 1998; Carr et al., 2003) or in response to prolonged high frequency trains of repetitive firing (Jung et al., 1997). Slow inactivation of sodium channels may be pivotal in regulating firing properties of a range of neurons by increasing spike threshold, curtailing prolonged action potential bursts and limiting active back propagation of action potentials into dendritic regions (Jung et al., 1997; Maurice et al., 2004). The last of these regulatory mechanisms may serve to dampen the excitability of dendrites by regulating NMDA receptor or voltage gated calcium channel mediated dendritic calcium spikes and hence could potentially affect processes such as spike timing dependent synaptic plasticity (Carr et al., 2003). Paroxysmal depolarising shifts associated with epileptiform cellular activity would present ideal conditions for the recruitment of this intrinsic inhibitory mechanism and pharmacological manipulation of this process would most likely have profound anticonvulsant effects. In support of this (Lees et al., 2006) we have previously shown that LCM exerts depressant effects on ictal-like events in rodent brain slices at concentrations (EC_{50s} circa 40-60 μ M) similar to those that significantly reduce sodium channel availability in this study.

Recently published studies suggest that certain opiate analgesics (Haeseler et al., 2006), carbamazepine (Cardenas et al., 2006) and a pre-clinical congener of DPH (Lenkowski et al.,

MOL #39867

2006) do to some extent promote slow inactivation of VGSCs in dorsal root ganglion cells or CNS neurons. However, upon examination of the voltage clamp experiments performed using these ligands it is apparent that they all concurrently interact with fast inactivation (in contrast to LCM). For example, the DPH analogue produced shifts in fast inactivation curves with pre-pulses that were as brief as 3 ms. LCM is the only anticonvulsant thus far, that appears to selectively promote slow sodium channel inactivation. The pre-clinical delta opiate agonist SNC80 has been elegantly demonstrated to exert effects on VGSC slow inactivation in acutely isolated hippocampal cells (Remy et al., 2004) but unlike with LCM, the rate of recovery from fast inactivation was also notably impaired.

Several studies have proposed potential structural correlates for slow inactivation, including changes in the configuration of the outer channel mouth (Xiong et al., 2003; Struyk and Cannon, 2002) and reduced efficiency of bending at the putative glycine gating hinge residue (Zhao et al., 2004) but the sub-molecular mechanism(s) of slow inactivation is (are) still poorly understood. LCM as a selective modifier of slow channel inactivation may be a useful tool to understand key domains on the VGSC that regulate availability by slow inactivation and to determine the pharmacophore for this novel modulatory mechanism.

The implications of selective promotion of slow inactivation for the pharmacological profile of such drugs *in vivo* have been investigated in animal experiments. The classical sodium channel modulating anticonvulsants are relatively inactive in the 6Hz psychomotor model of treatment resistant seizures (Barton et al., 2001) whilst LCM has shown full efficacy in this test (Beyreuther et al., 2007). Moreover, LCM has been compared to LTG in the streptozotocin model for diabetic neuropathic pain (Beyreuther et al., 2006). While LCM showed full efficacy against mechanical hyperalgesia and thermal allodynia, LTG was completely inactive. These results imply that selective enhancement of VGSC slow inactivation reported here and/or the novel interaction of LCM with cytoskeletal collapsin

MOL #39867

response mediator protein 2 (CRMP2: Beyreuther et al., 2007) can result in a distinct pharmacological profile when compared to drugs affecting fast inactivation of VGSCs as their primary mode of action.

In summary, our results suggest LCM does not share any of the mechanistic hallmarks of VGSC fast inactivation modifiers that have been used in epilepsy for some years. Instead, LCM alters the voltage dependence of the channel rearrangement underpinning slow inactivation as well as accelerating the process of entry into the slow inactivated state. Doses of LCM used in clinical trials yield plasma concentrations of 10 to 60 μM (Beyreuther et al., 2007; Doty et al., 2007) and we show that, at these concentrations, the drug produces sufficient modulation of sodium channel slow inactivation as to significantly constrain the ability of pyramidal neurons to sustain prolonged bursts (the hallmark of neurons in epileptic foci). This novel mechanism likely underpins the acute anticonvulsant and analgesic effects of the drug which are currently being profiled in clinical trials.

MOL #39867

Acknowledgments

The authors would like to acknowledge the contributions of Gareth Bruce, Marc Smith and Liping Huang who helped in production of neuronal cell cultures for this study and Kevin Markham for technical support.

MOL #39867

Reference List

- Barton ME, Klein BD, Wolf HH, White HS (2001) Pharmacological characterization of the 6 Hz psychomotor seizure model of partial epilepsy. *Epilepsy Res* **47**:217-227.
- Beyreuther B, Callizot N, Stöhr T (2006) Antinociceptive efficacy of lacosamide in a rat model for painful diabetic neuropathy. *Eur J Pharmacol* **539**:64-70.
- Beyreuther BK, Freitag J, Heers C, Krebsfaenger N, Scharfenecker U, Stöhr T (2007) Lacosamide: A review of preclinical properties. *CNS Drug Rev.* **13**(1):21-42
- Cardenas CA, Cardenas CG, de Armendi AJ, and Scroggs (2006) Carbamazepine interacts with a slow inactivation state of Na_v1.8-like sodium channels. *Neurosci Lett* **408**, 129-134
- Carr DB, Day M, Cantrell A R, Held J, Scheuer T, Catterall W A and Surmeier D J (2003) Transmitter Modulation of Slow, Activity-Dependent Alterations in Sodium Channel Availability Endows Neurons With a Novel Form of Cellular Plasticity. *Neuron* **39**:793-806.
- Cunningham MO and Jones RSG (2000) Lamotrigine decreases spontaneous glutamate release and increases GABA release in the rat entorhinal cortex *in vitro*. *Neuropharmacology* **39**, 2139-2146.
- Doty P, Rudd GD, Stöhr T and Thomas D (2007) Lacosamide. *Neurotherapeutics* **4**:145-148.
- Errington AC, Coyne L, Stöhr T, Selve N and Lees G (2006) Seeking a Mechanism of Action for the Novel Anticonvulsant Lacosamide. *Neuropharmacology* **50**:1016-1029.
- Haeseler G, Foadi N, Ahrens J, Dengler R, Hecker H and Leuwer M (2006). Tramadol, fentanyl and sufentanil but not morphine block voltage-operated sodium channels. *Pain* **126** 234-244.

MOL #39867

Jung H Y, Mickus T, and Spruston N (1997) Prolonged sodium channel inactivation contributes to dendritic action potential attenuation in hippocampal pyramidal neurons. *J Neurosci* **17** (17), 6639-6646

Kuo CC and Bean B P (1994) Slow Binding of Phenytoin to Inactivated Sodium Channels in Rat Hippocampal Neurons. *Mol Pharmacol* **46**:716-725.

Kuo CC, Chen R S, Lu L and Chen R C (1997) Carbamazepine Inhibition of Neuronal Na⁺ Currents: Quantitative Distinction From Phenytoin and Possible Therapeutic Implications. *Mol Pharmacol* **51**:1077-1083.

Kuo CC and Lu L (1997) Characterization of Lamotrigine Inhibition of Na⁺ Channels in Rat Hippocampal Neurons. *Br J Pharmacol* **121**:1231-1238.

Kuo CC (1998) A Common Anticonvulsant Binding Site for Phenytoin, Carbamazepine, and Lamotrigine in Neuronal Na⁺ Channels. *Mol Pharmacol* **54**:712-721.

Lang DG, Wang C M and Cooper B R (1993) Lamotrigine, Phenytoin and Carbamazepine Interactions on the Sodium Current Present in N4TG1 Mouse Neuroblastoma Cells. *J Pharmacol Exp Ther* **266**:829-834.

Lees G and Leach M J (1993) Studies on the Mechanism of Action of the Novel Anticonvulsant Lamotrigine (Lamictal) Using Primary Neurological Cultures From Rat Cortex. *Brain Res* **612**:190-199.

Lees G, Stohr T and Errington A C (2006) Stereoselective Effects of the Novel Anticonvulsant Lacosamide Against 4-AP Induced Epileptiform Activity in Rat Visual Cortex in Vitro. *Neuropharmacology* **50**:98-110.

MOL #39867

Lenkowski PW, Batts TW, Smith MD, Ko SH, Jones PJ, Taylor CH, McCusker AK, Davis GC, Hartman HA, White HS, Brown ML and Patel MK (2006) A Pharmacophore derived Phenytoin Analogue with Increased Affinity for Slow Inactivated Sodium Channels exhibits a desired Anticonvulsant Profile. *Neuropharmacology* **52**: 1044-1054

LeTiran A, Stables J P and Kohn H (2001) Functionalized Amino Acid Anticonvulsants: Synthesis and Pharmacological Evaluation of Conformationally Restricted Analogues. *Bioorg Med Chem* **9**:2693-2708.

Maurice N, Mercer J, Chan C S, Hernandez-Lopez S, Held J, Tkatch T and Surmeier D J (2004). D2 Dopamine Receptor-Mediated Modulation of Voltage-Dependent Na⁺ Channels Reduces Autonomous Activity in Striatal Cholinergic Interneurons. *J Neurosci* **24** (46), 10289-10301

McCleane G, Koch B and Rauschkolb C (2004) Does SPM 927 Have an Analgesic Effect in Human Neuropathic Pain? An Open Label Study. *Neurosci Letters* **352**:117-120.

McLean MJ and McDonald R L (1986) Multiple Actions of Phenytoin on Mouse Spinal Cord Neurons in Cell Culture. *J Pharmacol Exp Ther* **237**:779-789.

McPhee JC, Ragsdale D S, Scheuer T and Catterall W A (1995) A Critical Role for Transmembrane Segment IVS6 of the Sodium Channel α Subunit in Fast Inactivation. *J Biol Chem* **270**:12025-12034.

Meldrum B (2002) Do Preclinical Seizure Models Preselect Certain Adverse Effects of Antiepileptic Drugs. *Epilepsy Res* **50**:33-40.

Mickus T, Jung H Y and Spruston N, (1999) Slow sodium channel inactivation in CA1 pyramidal cells. *Annals Of The New York Academy Of Sciences* **868** 97-101

MOL #39867

Miller AA, Wheatly P, Sawyer D A, Baxter M G and Roth B (1986) Pharmacological Studies on Lamotrigine, a Novel Potential Antiepileptic Drug: I. Anticonvulsant Profile in Mice and Rats. *Epilepsia* **27**:483-489.

Poolos NP, Migliore M, Johnston D (2002) Pharmacological upregulation of h-channels reduces the excitability of pyramidal neuron dendrites. *Nature Neuroscience* **5** (8), 767-774.

Quandt FN (1988) Modification of Slow Inactivation of Single Sodium Channels by Phenytoin in Neuroblastoma Cells. *Mol Pharmacol* **34** (4), 557-565

Ragsdale DS, McPhee J C, Scheuer T and Catterall W A (1996) Common Molecular Determinants of Local Anesthetic, Antiarrhythmic and Anticonvulsant Block of Voltage Gated Na Channels. *Proc Natl Acad Sci USA* **93**:9270-9275.

Ragsdale DS and Avoli M (1998) Sodium Channels As Molecular Targets for Antiepileptic Drugs. *Brain Res Rev* **26**:16-28.

Remy C, Remy S, Beck H, Swandulla D, and Hans M (2004) Modulation of voltage-dependent sodium channels by the δ -agonist SNC80 in acutely isolated rat hippocampal neurons. *Neuropharmacology* **47** (7) 1102-1112.

Ridall DR, Leach MJ, Garthwaite J (2006) A novel drug binding site on voltage-gated sodium channels in rat brain. *Mol Pharmacol* **69** (1) 278-287.

Rudy B (1978) Slow inactivation of the sodium conductance in squid giant axons. Pronase resistance. *J Physiol* **283**:1-21

Struyk A F and Cannon SC (2002) Slow Inactivation Does Not Block the Aqueous Accessibility to the Outer Pore of Voltage-Gated Na Channels. *J Gen Physiol* **120** (4): 509-516

MOL #39867

Toib A, Lyakhov V and Marom S (1998) Interaction Between Duration of Activity and Time Course of Recovery from Slow Inactivation in Mammalian Brain Na⁺ Channels. *J Neurosci* **18** (5):1893-1903

Vedantham V and Cannon SC (1999) The position of the fast inactivation gate during lidocaine block of voltage-gated Na⁺ channels. *J. Gen Physiol* **113**: 7-16.

Wang CM, Lang D G and Cooper B R (1993) Lamotrigine Effects on Ion Channels in Neuronal Cells. *Epilepsia* **34**:117-118.

Willow M, Gonoï T and Catterall W A (1985) Voltage Clamp Analysis of the Inhibitory Actions of Diphenylhydantoin and Carbamazepine on Voltage-Sensitive Sodium Channels in Neuroblastoma Cells. *Mol Pharmacol* **27**:549-558.

Xiong W, Li RA, Tian Y and Tomaselli GF (2003) Molecular Motions of the Outer Ring of Charge of the Sodium Channel: Do They Couple to Slow Inactivation? *J Gen Physiol* **122** (3): 323-332.

Zhao Y, Yarov-Yarovoy V, Scheuer T and Catterall WA (2004) A Gating Hinge in Na⁺ Channels: A Molecular Switch for Electrical Signaling. *Neuron* **41** (6): 859-865.

MOL #39867

Footnotes

The Otago project (consumables and electrophysiological apparatus) and ACEs studentship was funded by Schwarz BioSciences GmbH, Monheim, Germany. LCM and SPM6953 were supplied by Schwarz Pharma GmbH (Monheim, Germany).

Some of the data presented here have been or will be published in meetings abstracts:-

Epilepsia 47: 84-85 Suppl 3 2006

Proceedings of the Society for Neuroscience (San Diego meeting November 2007)

Reprint requests to:

Professor George Lees PhD FRPharmS

Chair, Department of Pharmacology & Toxicology

Otago School of Medical Sciences

University of Otago

PO Box 913

Dunedin, New Zealand

george.lees@stonebow.otago.ac.nz

MOL #39867

Legends for figures

Figure 1. (A) Functionalised amino acid structure of the novel anticonvulsant molecule LCM (R-2-acetamido-N-benzyl-3-methoxypropionamide). The asterisk indicates the chiral centre: the R isomer LCM is biologically active whilst the L isomer (SPM6953) had no significant effect in pre-clinical epilepsy models **(B)** DPH **(C)** CBZ **(D)** LTG.

Figure 2. (A) Current profiles evoked in cultured cortical neurons by a fast ramp depolarisation of the holding potential from -70 to 20 mV (90 mV/sec). Prior to drug treatment high frequency bursts of TTX-sensitive (not shown) action currents were observed. CBZ (100 μ M) and DPH (100 μ M) produced profound and reversible inhibition of spike firing. LCM (100 μ M) had only a weak effect on the frequency of spikes induced by fast ramps. **(B)** Histograms showing the marked reduction in spike frequency produced by CBZ and DPH (in contrast to the moderate effect of LCM) and the increased latency to first spike in the presence of these drugs. **(D)** Spikes evoked by slow depolarising ramps were weakly sensitive to inhibition by LCM but were completely occluded by CBZ and DPH (all at 100 μ M) as summarised in **(C)**.

Figure 3 (A) Representative experiment showing concentration dependent inhibition of action potential firing in ten second bursts of evoked SRF in a single cell pyramidal neuron with a resting potential of -70 mV (Bottom trace). Mean firing frequency plot in 10 s bins. (Top) **(B)** Overlaid mean frequency plots (1 s bins) showing the inhibition of firing by LCM. The open portion reflects the control frequency. Light grey demonstrates the conversion of the firing pattern to that of interrupted repetitive firing (or bursting) by 32 μ M LCM that can also be seen in the expanded tracing shown in D. The black portion shows the profound effect of

MOL #39867

320 μM LCM. Note here however that although the duration of the repetitive firing is markedly attenuated the initial frequency (in the first second) is virtually unchanged. **(C)** Concentration-response curves for the data as analysed in A (10 s bins, open squares) and in B (1 s bins, closed squares). Note the profound shift in potency for prolonged evoked trains **(D)** Expanded representative tracings of the 10 s SRF showing the inhibitory effects of LCM. The inset histogram displays the residual duration of firing at equilibrium. **(E)** In marked contrast to LCM the other antiepileptic drugs CBZ, LTG and DPH inhibit all spikes except those occurring within approximately 100 ms of the burst initiation.

Figure 4 (A) Families of current responses to a 10 ms depolarising step (-60 to +110 mV) from a representative cell before and after application of 100 μM LCM. Inset shows the complete block of the evoked inward current by tetrodotoxin (0.5 μM). Note the presence of a TTX-sensitive persistent sodium current in these cells. **(B)** Current-voltage plot taken from a different cell to that shown in A demonstrates the reversal potential (*) is close to the predicted Nernstian Na^+ equilibrium potential and that LCM reversibly blocked both inward and outward sodium currents. After removal of the drug the curve was almost coincident with the pre-treatment curve in this cell. Inset: the step depolarisation protocol used to evoke currents. **(C)** Representative normalized conductance-voltage plot from a single cell (different to those used in A,B) showing that curves were almost super-imposable in the presence of LCM and in control. The box and whisker plot shows the V_{50} for activation was not significantly shifted ($P > 0.05$, Mann-Whitney) in replicated experiments ($n = 4$). This confirms that the block by LCM did not reflect shifts in the voltage dependence of activation gating. **(D)** The target for LCM is stereoselective. Families of evoked currents were not altered by SPM 6953 (100 μM) compared to pre-treatment currents. The maximal current evoked using the inset pulse protocol was reduced by LCM but not by SPM 6953 (which is

MOL #39867

not anticonvulsant *in vivo*). The effect of 100 μ M LCM in reducing sodium currents was significantly ($P > 0.05$, $n = 3$) different to an equal concentration of the S-stereoisomer.

Figure 5 (A) LCM (top) produced inhibition of transient sodium currents evoked by test pulses to 0 mV from a holding potential of -60 mV with (left) or without (right) a prior 500 ms hyperpolarizing prepulse. In contrast, the blocking effect of DPH (bottom right) could be completely occluded (traces overlaid, bottom left) by the hyperpolarising pulses. (B) Bar chart summarising the profound voltage dependent blocking action of the typical sodium channel acting anticonvulsants CBZ, LTG and DPH in the same experiment. All three anticonvulsants produced marked inhibition of currents evoked from -60 mV that was considerably reduced when a 500 ms hyperpolarising pulse was delivered prior to the test pulse. LCM on the other hand produced approximately 30 % reduction in current under both conditions (C) The frequency-dependence of block was examined from a relatively hyperpolarised holding potential and currents were evoked at 10 Hz by 20 ms test pulses to -10 mV (protocol shown inset, below). Representative overlaid current traces are shown of the 1st, 10th, 20th and 30th pulses under control conditions and in the presence (right) of DPH and LCM. (D) Plot summarising the frequency dependent decrement in peak current amplitude (mean value from replicated experiments) produced by CBZ, LTG and DPH but not LCM (for clarity error bars are not shown, values are quoted in text). A small decrement ($\sim 10\%$) in peak current amplitude was observed under control conditions (open squares). After only ten pulses both CBZ and DPH produced significantly more attenuation of current than pre-treatment (LTG followed the trend). At the end of the thirty pulse train all three anticonvulsants produced significant inhibition compared to pre-treatment. In contrast, 100 μ M LCM exerted no significant ($P > 0.05$) frequency dependent facilitation of block even after 30 pulses, although

MOL #39867

a slow reduction in the peak current was observed beginning after approximately 12-13 pulses (*arrow*).

Figure 6. (A) Steady state inactivation curves before and after equilibration with anticonvulsant drugs. Prepulses (500 ms) between -120 and -20 mV were given followed immediately by a test pulse (30 ms) to -10 mV (A *inset*). Tracings showing voltage dependent steady state fast inactivation of sodium currents and the effects of CBZ and LCM. (B) Steady state fast inactivation curves (Boltzman fit) were shifted in the hyperpolarizing direction by CBZ, LTG and DPH (note that the LTG and DPH curves and data points are almost superimposed) but not by LCM compared to pooled control data ($n = 21$). (C) Box and whisker plot showing the V_{50} for inactivation was significantly ($P < 0.05$, Kruskal-Wallis with Dunn's multiple comparison test *post hoc*) shifted in the hyperpolarizing direction for CBZ ($P < 0.001$, $n = 5$), LTG ($P < 0.05$, $n = 7$) and DPH ($P < 0.05$, $n = 7$) but not LCM ($P > 0.05$, $n = 7$) compared to control data. LCM appeared to produce a marginal depolarising shift in steady state inactivation. V_{50} for inactivation in the presence of LCM was not statistically altered compared to controls ($P > 0.05$) but the slope of the curve was identical and all points were displaced to the right across the replicated experiments. (D) Currents depicting recovery from fast inactivation were measured using the pulse protocol illustrated in the absence and presence of drugs (Δt is indicated in ms for each trace). (E) Plot of the recovery in presence and absence of drugs. Note that recovery was 95 % complete after 100 ms in control saline. (F) CBZ (100 μM ; grey bars) significantly prolonged the time for recovery from steady state fast inactivation ($P < 0.001$). LCM (100 μM ; black bars) did not alter the time for recovery significantly ($P > 0.05$) or displace the control curve (white bars) compared to the obvious retardation of recovery with CBZ.

Figure 7. LCM enhances the entry of sodium channels into the slow inactivated state. (A) Under drug-free physiological conditions the pulse protocol used (*inset*, 10 s) resulted in

MOL #39867

reduced channel availability ($P2 / P1$) of approximately 30 % in voltage-clamped N1E 115 cells. The extent of physiological slow inactivation was consistent across three different groups of cells. LCM produced a concentration dependent enhancement in the reduction of sodium channel availability attributable to slow inactivation. **(B)** Plot of the fraction of current unavailable as a result of physiological slow inactivation (open circles, n indicated) for each group of cells compared to the fraction unavailable in the presence of increasing concentration of (LCM 32-320 μM , filled circles). To account for the tonic blocking action of LCM at the holding potential used, the enhancement of slow inactivation was measured as the fraction of current made unavailable after the conditioning pulse ($P2_{\text{LCM}}$) compared to that available before conditioning ($P1_{\text{LCM}}$) in the presence of the drug. **(C)** Concentration response curves for the inhibition of sodium currents by LCM at the holding potential of -80 mV ($P1_{\text{LCM}} / P1_{\text{CONT}}$, open squares) and after slow inactivation was induced by the conditioning pulse to -20 mV ($P2_{\text{LCM}} / P2_{\text{CONT}}$, closed squares). LCM produced a greater (but not significant $P > 0.05$, $n = 5-7$, Mann Whitney) reduction in the peak current amplitude in cells where slow inactivation was prevalent. **(D)** LCM enhances the rate of entry of sodium channels into the unavailable slow inactivated state with time constants for entry as shown. The first data points were taken from the recovery experiments presented in figure 6DE and represents the fraction of current available after a one second recovery period from a 500 ms conditioning pulse.

Figure 8. **(A)** In a concentration-dependent manner LCM shifted the voltage dependence of slow inactivation of sodium currents. Tracings show the voltage dependence of slow inactivation under pre-treatment (top) and LCM treated conditions (bottom). The fraction of peak current available in response to a test pulse to -10 mV was significantly reduced by 100 μM LCM across the range of potentials from -80 to -10 mV. In the presence of LCM 100 μM (open squares) the slow inactivation voltage curve was significantly shifted ($P < 0.001$, $n = 4-8$, Friedman with Dunn's multiple comparison) to more hyperpolarized potentials. The

MOL #39867

normalised peak amplitude of whole cell currents evoked after depolarizing conditioning pulses were clearly reduced in the presence of the drug compared to the currents evoked after the same depolarizing conditioning pulse pre-treatment (closed squares). **(B)** Tracings show progressive recovery of sodium current from slow inactivation in control (top) and LCM (100 μ M, bottom) treated conditions. The fraction of channels made unavailable by slow inactivation was significantly enhanced by LCM but the half-life for channel recovery (τ) was not significantly changed (τ values derived from mono-exponential curve fits are shown; ns indicates $P > 0.05$). **(C)** Tracing shows recovery of sodium currents in the presence of 100 μ M CBZ ($n = 3$, open circles) from slow inactivation induced using pulse protocol shown in B. Unlike the effects of LCM, CBZ did not enhance the fraction of channels made unavailable by running the slow inactivation protocol. The peak current available after the conditioning pulse was in fact slightly greater in the presence of CBZ than control conditions (closed squares).

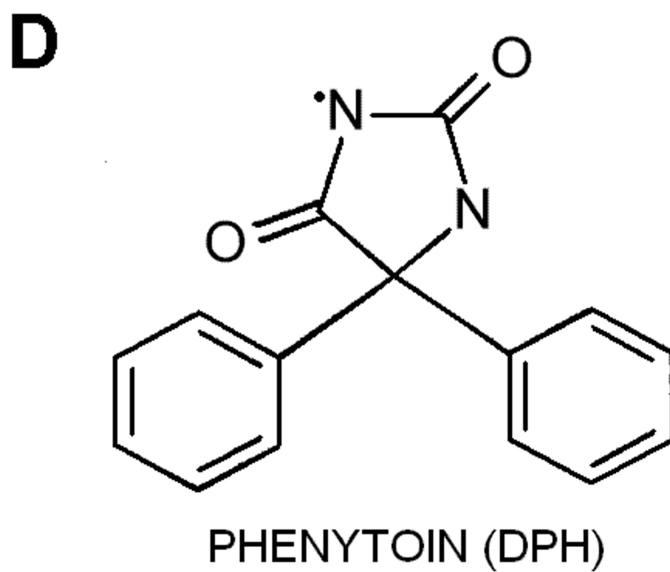
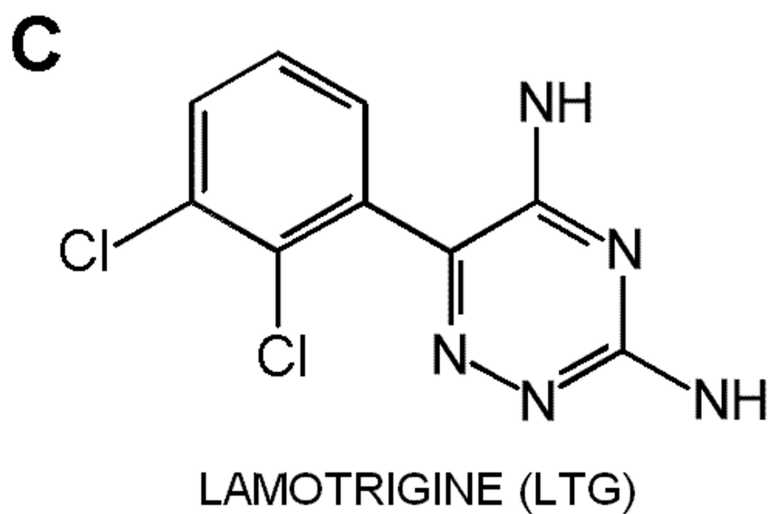
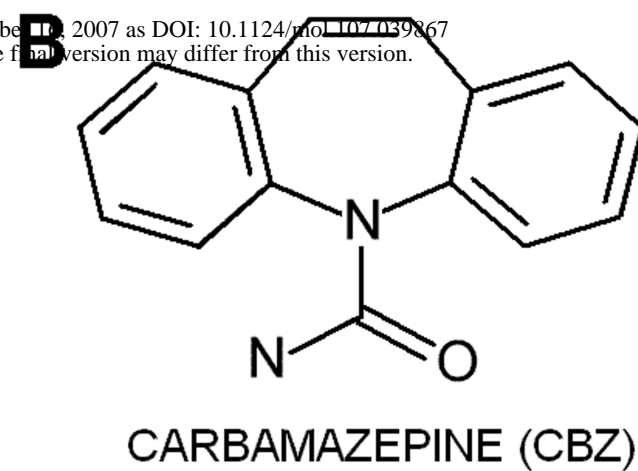
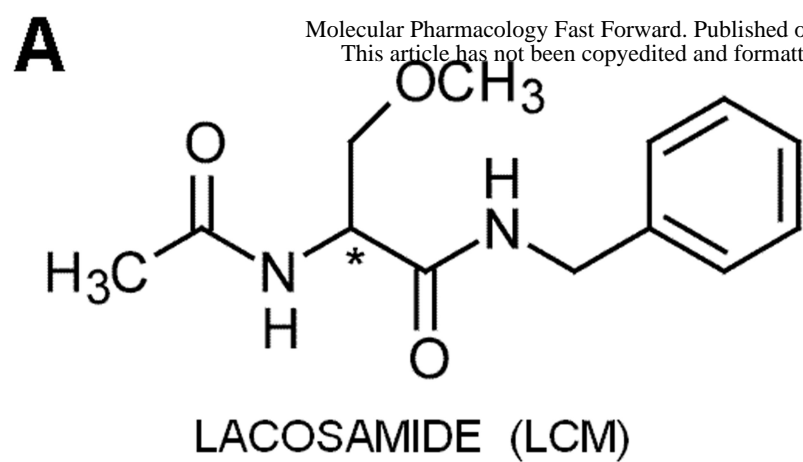


Figure 1

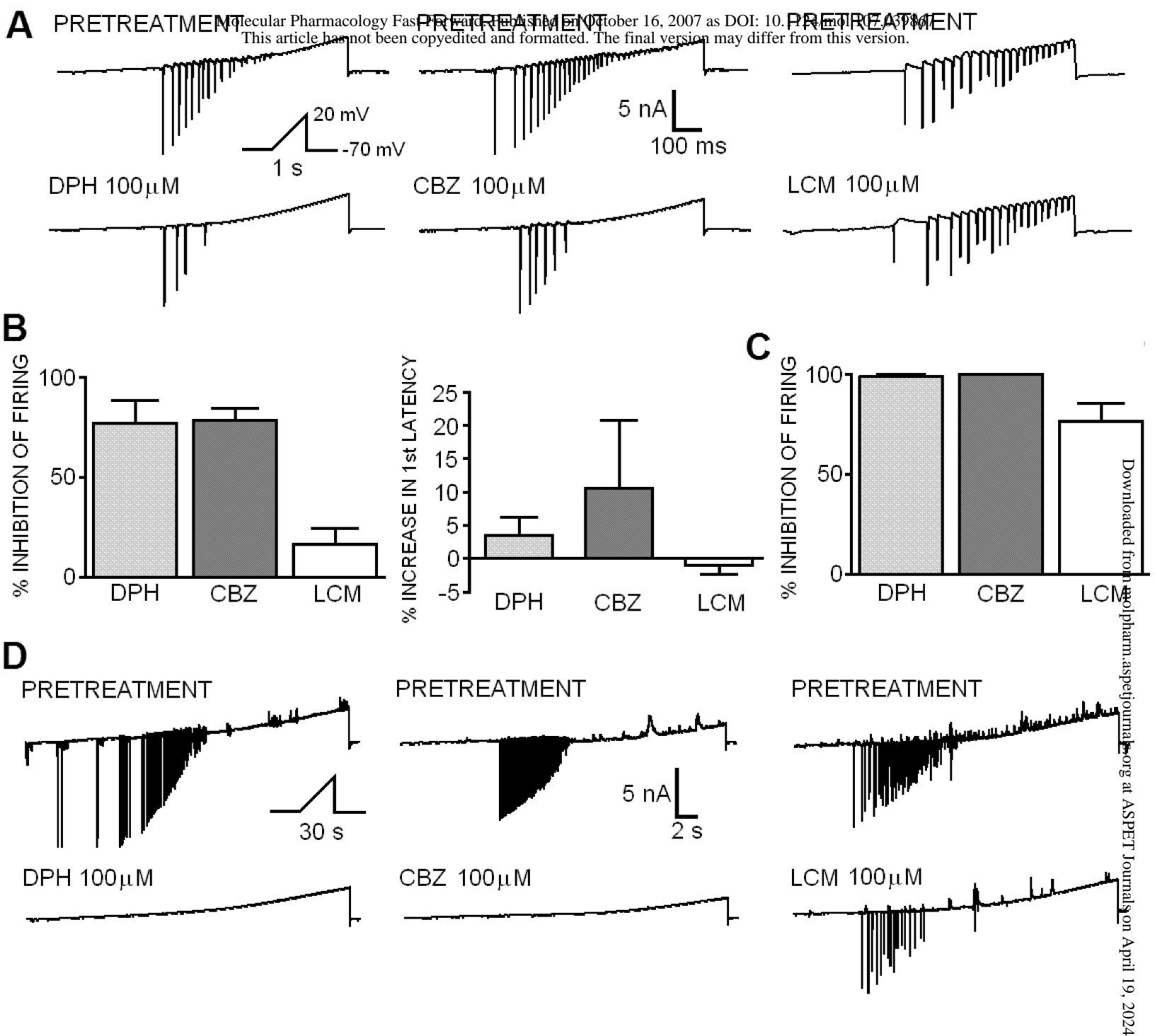


Figure 2

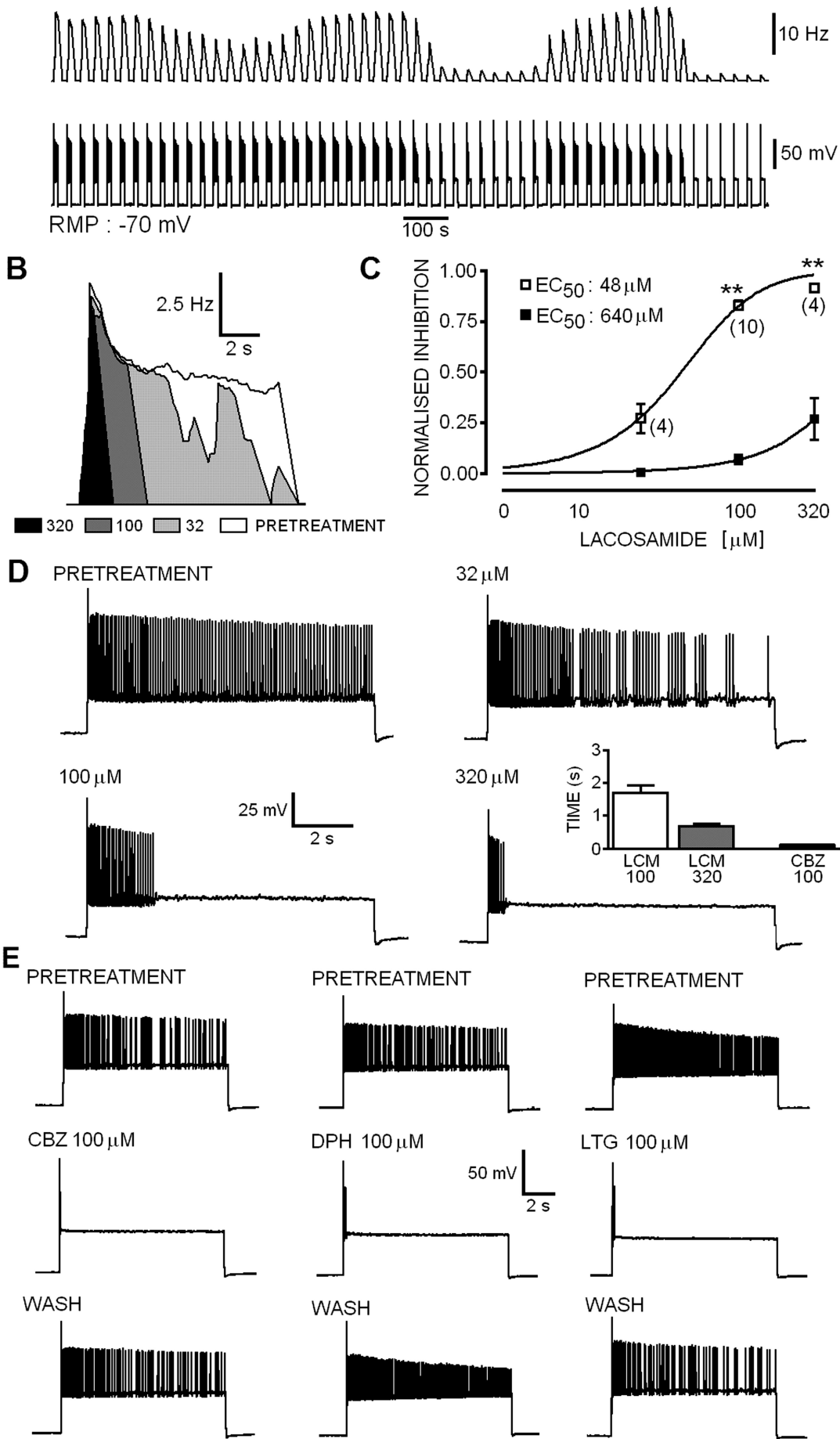


Figure 3

A PRETREATMENT LCM 100 μM

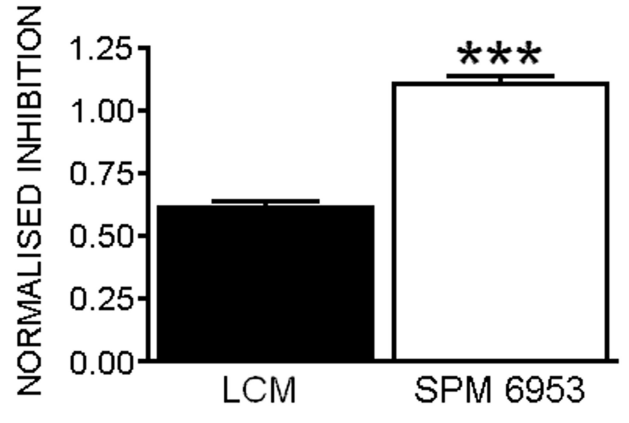
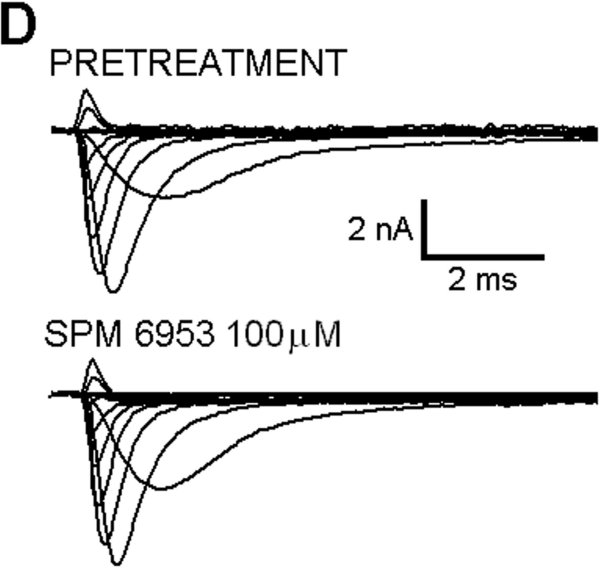
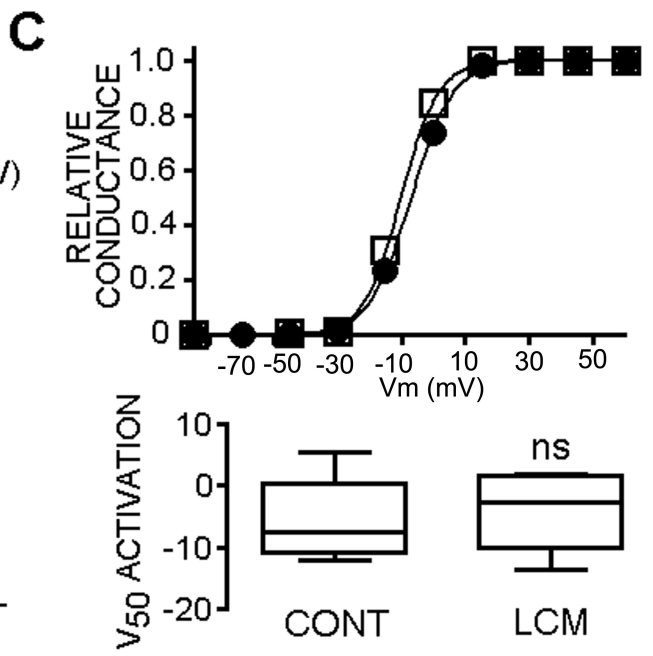
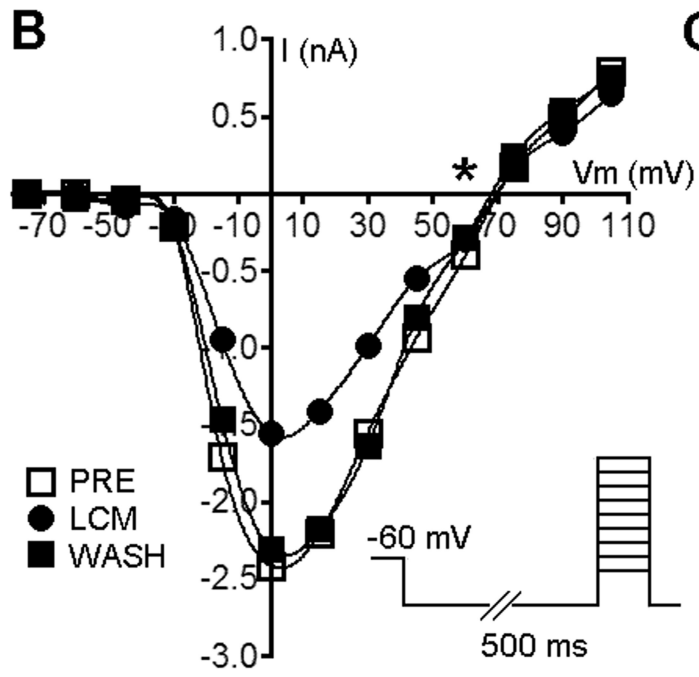
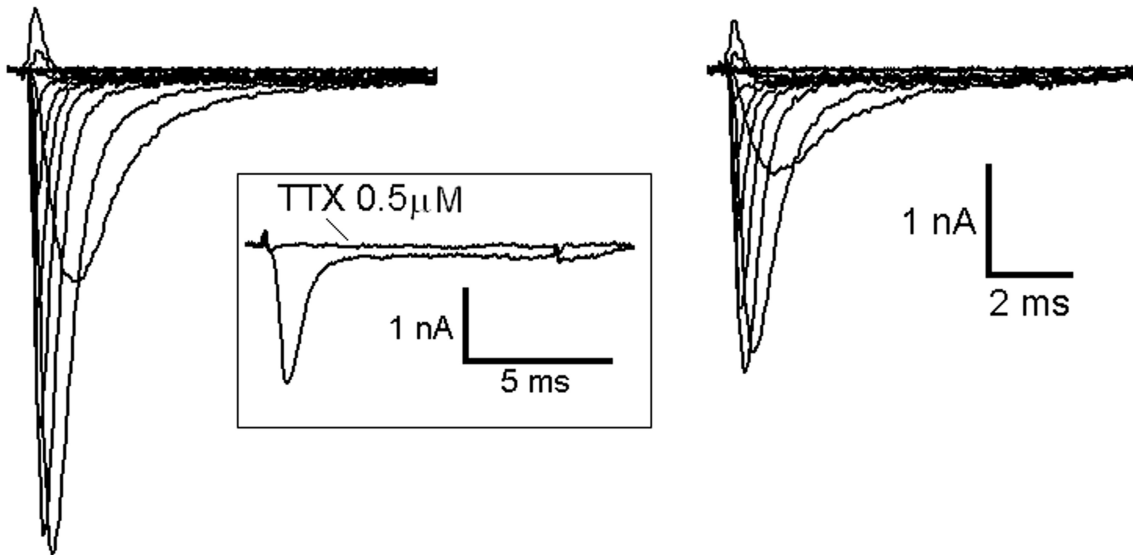


Figure 4

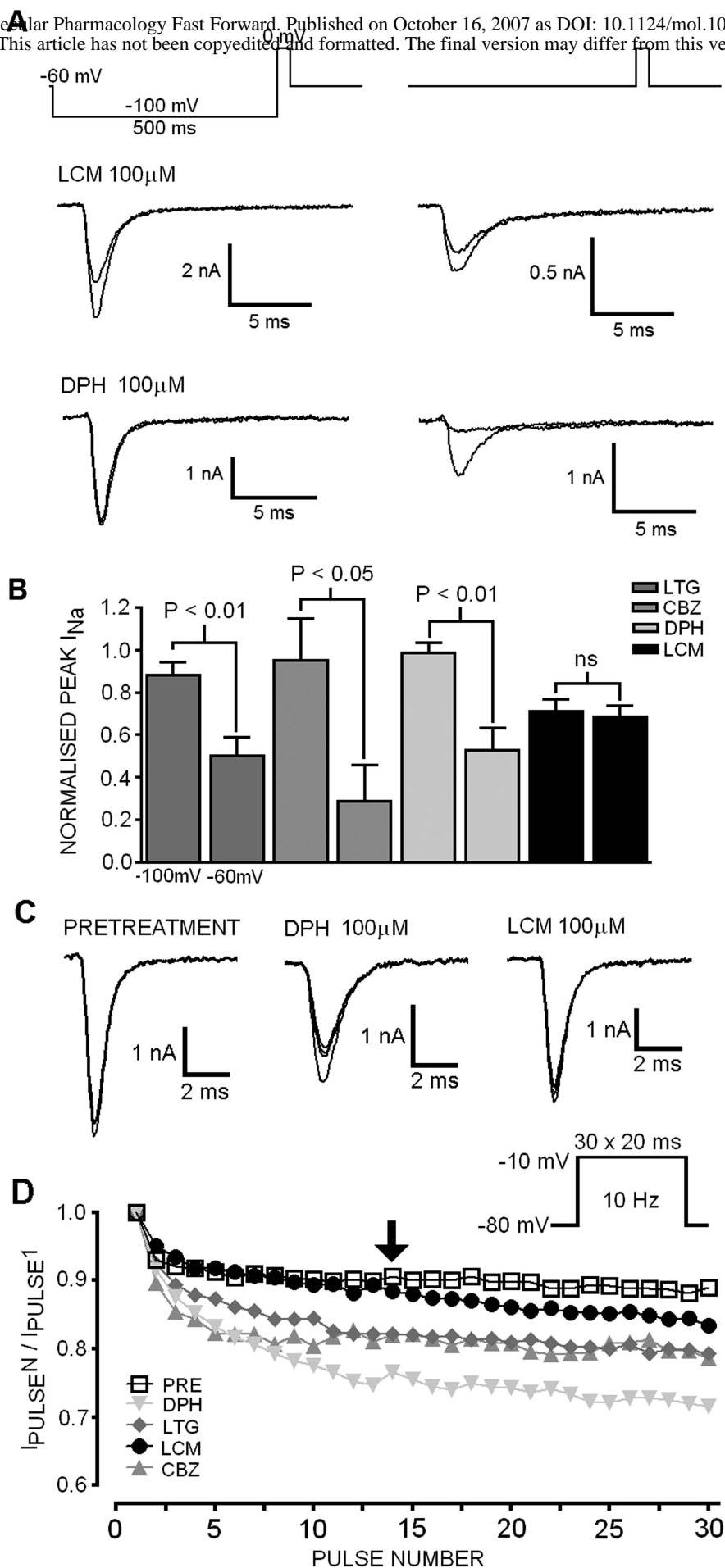


Figure 5

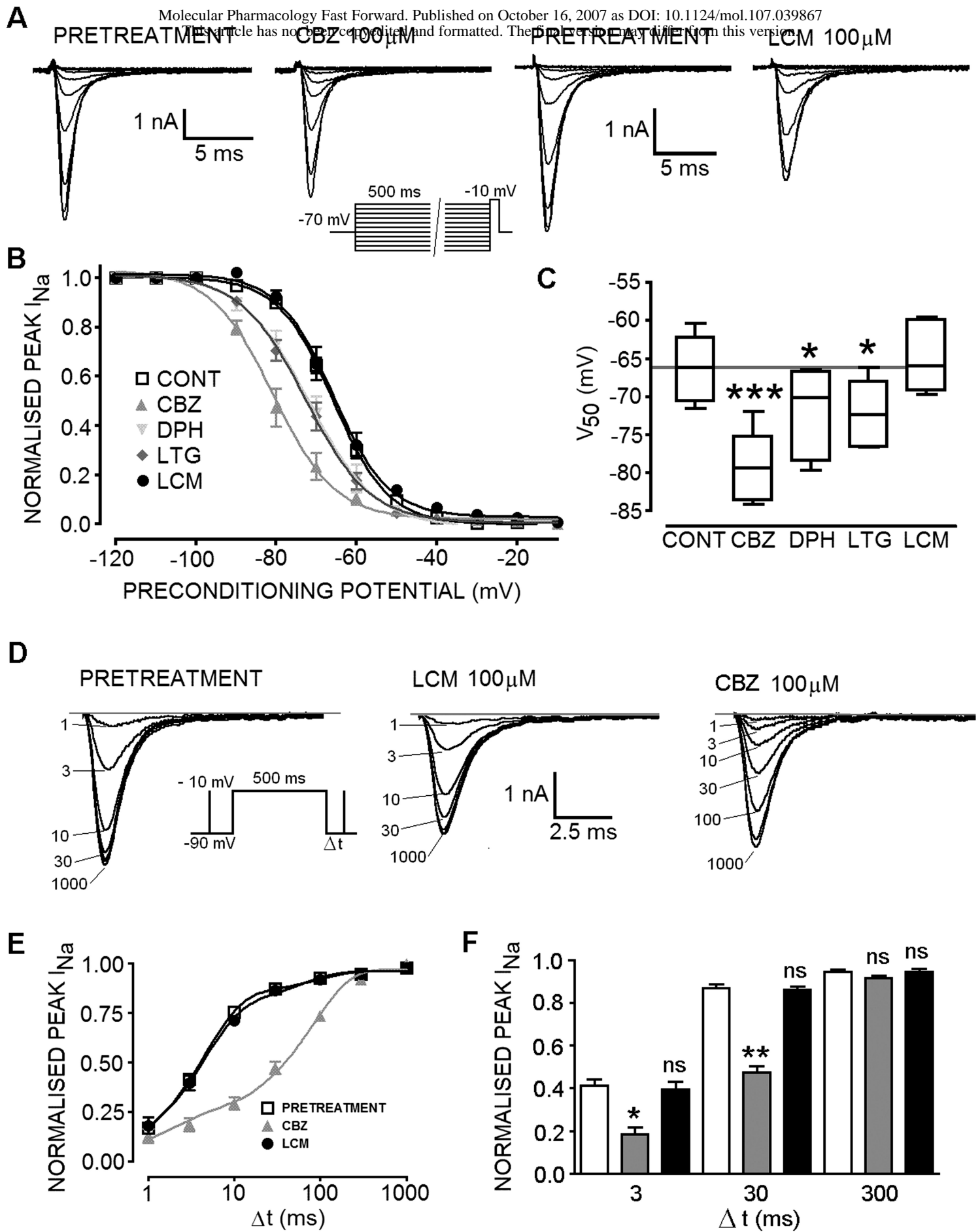


Figure 6

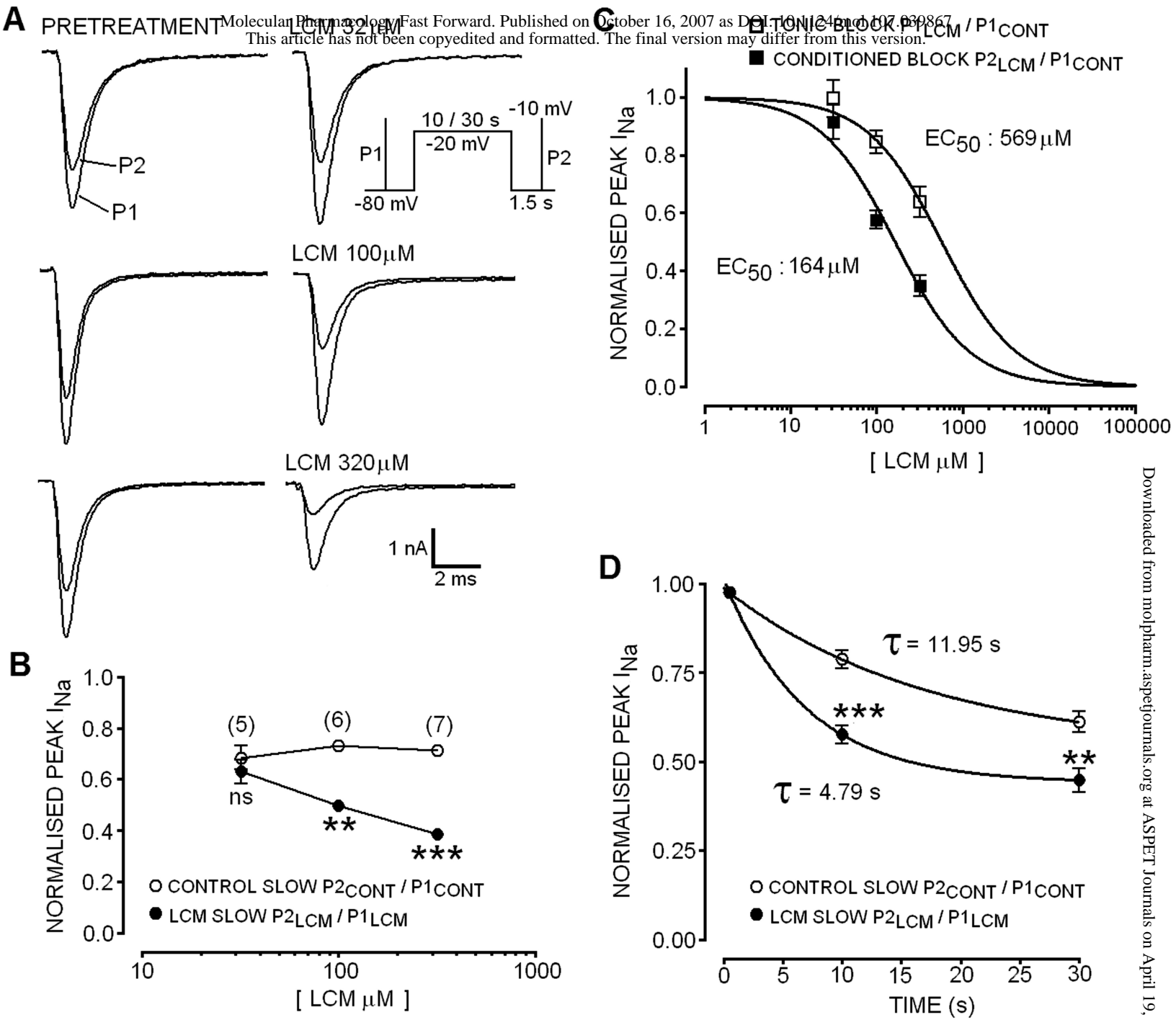


Figure 7

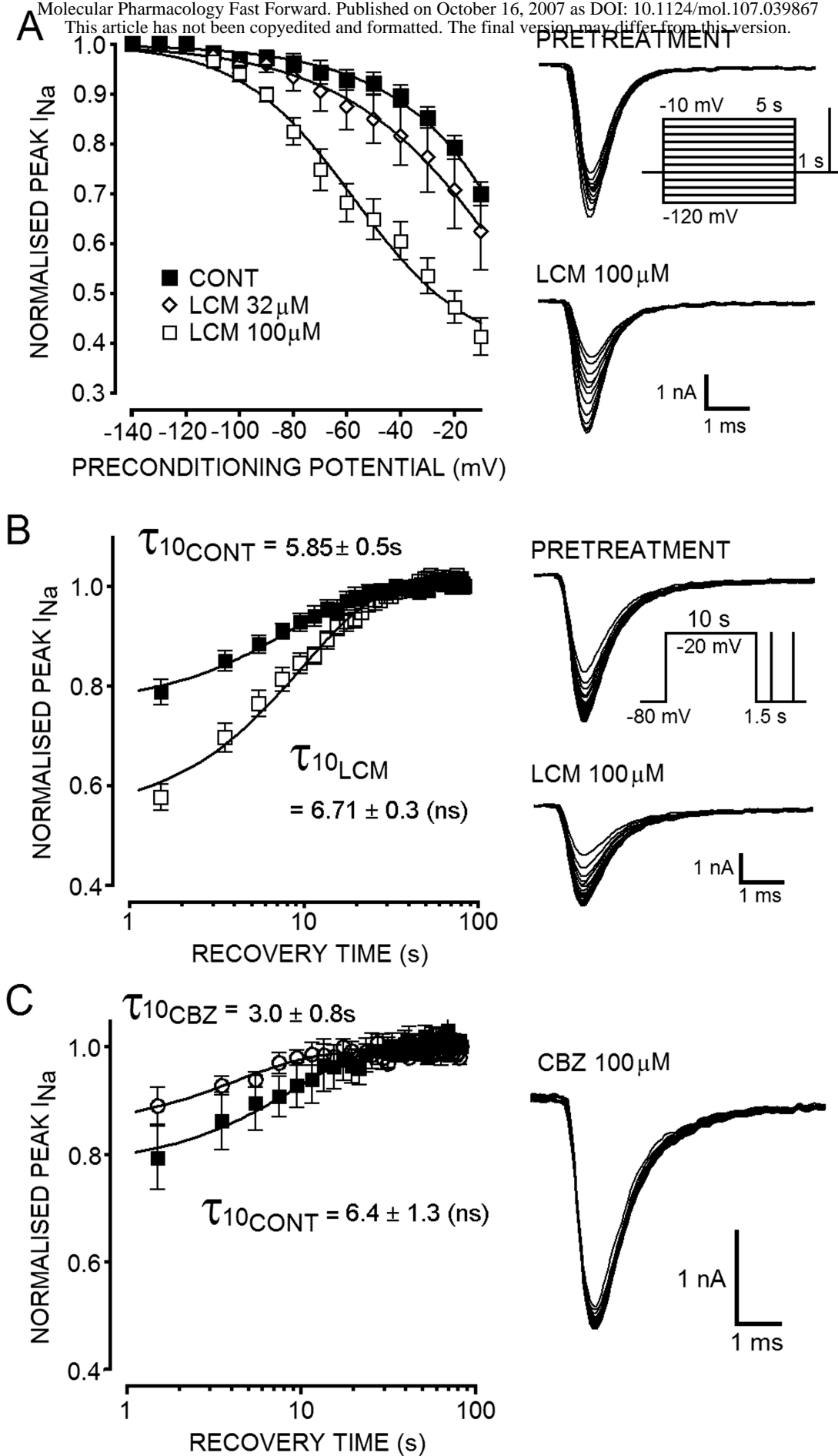


Figure 8